ACS APPLIED ENERGY MATERIALS

www.acsaem.org Article

Designing Polyurethane Solid Polymer Electrolytes for High-Temperature Lithium Metal Batteries

Rassmus Andersson, Guiomar Hernández, Jennifer See, Tony D. Flaim, Daniel Brandell, and Jonas Mindemark*

Cite This: *ACS Appl. Energy Mater.* 2022, 5, 407−418 Read Online

ACCESS | Metrics & More | Article Recommendations | Supporting Information

ABSTRACT: Potentially high-performance lithium metal cells in extreme high-temperature electrochemical environments is a challenging but attractive battery concept that requires stable and robust electrolytes to avoid severely limiting lifetimes of the cells. Here, the properties of tailored polyester and polycarbonate diols as the soft segments in polyurethanes are investigated and electrochemically evaluated for use as solid polymer electrolytes in lithium metal batteries. The polyurethanes demonstrate high mechanical stability against deformation at low flow rates and moreover at temperatures up above 100 °C, enabled by the hard urethane segments. The results further indicate transferrable ion transport properties of the pure polymers when incorporated as the soft segments in the polyurethanes, offering designing opportunities of the polyurethane by tuning the soft segment ratio and composition. Long-term electrochemical cycling of polyurethane-containing cells in lithium metal batteries at 80 °C proves the stability at elevated temperatures as well as the compatibility with lithium metal with stable cycling maintained after 2000 cycles.

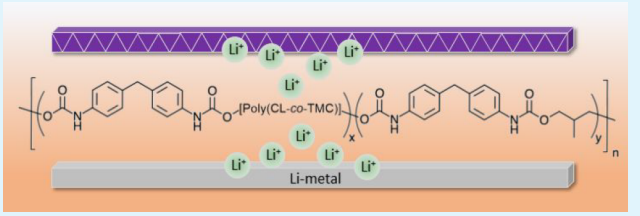

KEYWORDS: *polymer electrolytes, high-temperature batteries, polyurethane, lithium metal batteries, long-term cycling*

INTRODUCTION

Simultaneously to the increasing demand for high-energy-density Li-ion batteries (LIBs), the need for high-temperature battery operation is likewise on the rise. Large markets where the LIBs are required to endure high-temperature operations are, for example, the oil, gas, and military industries.[1−3] High-temperature LIBs are also of great interest for the electrical vehicle (EV) market since they will enable the possibility for more energy-efficient operations by reducing the requirements on large and heavy energy-consuming cooling systems.[4] At the same time, the intercalation chemistry in LIBs is approaching its inherent limits in terms of capacity, prompting efforts into the study of other battery chemistries.[3,5−7]

One way to increase the energy density is to replace the conventional graphite-based anode with lithium metal, which has a low reduction potential and much higher capacity.[8] The use of lithium metal as the anode material does, however, come with the safety issues of high reactivity as well as dendrite growth through the electrolyte. By replacing the liquid electrolyte with a solid polymer electrolyte (SPE), not only can the dendrite growth be prevented but the safety issues associated with the volatile and flammable liquid electrolyte can also be avoided. SPEs possess the unique characteristics of having a low flammability, good processability and flexibility, and great thermal stability.[9−13] The main disadvantage of SPEs is their ionic conductivity, which typically is 2−3 orders of magnitude lower than for liquid electrolytes. The origin is to be found in the slower ion transport mechanism in SPEs assisted by polymer segmental motions compared to vehicular transport in liquid electrolytes.[11−14]

Compared to liquid counterparts, the mechanical and thermal stability of SPEs is improved. At elevated temperatures, however, most of the reported SPEs are suffering from stability issues.[15,16] Therefore, there is a trade-off between conductivity and stability, which both are influenced by temperature. SPEs should hence be both flexible to conduct ions, while they must be mechanically stable to tolerate the strains and prevent the dendrite growth the battery is exposed to during operation.

A careful design of the SPE is critical to achieve an adequately performing lithium battery,[17] especially at elevated temperatures. Inherent parameters of the SPE that strongly influence its performance are, among others, the salt content which normally affects the glass transition temperature (T_g), the crystallinity of the SPE, the mechanical stability, and the ionic conductivity.[18−20] Efforts that have been implemented to promote the performance by increasing the mechanical stability or ionic conductivity, or both, are through cross-linking the polymer,[21,22] incorporating fillers and nanoparticles

Received: September 20, 2021
Accepted: December 22, 2021
Published: January 10, 2022

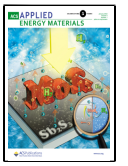

into the polymer matrix,[23−26] decreasing the molecular weight,[27,28] utilizing single-ion polymer electrolytes,[29,30] and copolymer electrolytes.[31,32] Another route to enhance the performance is to employ block copolymer electrolytes in SPEs, in which each block contributes with different attributes to the overall behavior. Normally, at least one block contributes with good ionic conductivity properties, while at least one block is rigid and supplies the mechanical stability.[33−36]

Polyurethanes constitute a type of polymer that consists of two continuous alternating components in the structure: one hard urethane segment and one soft segment. There is wide variety in the choice of the soft segment which can be synthesized prior to the formation of the polyurethane structure. The properties of the soft segment can therefore to a large extent be designed to meet specific application requirements.[37] In the context of SPEs, this would correspond to a cation-coordinating soft polymer with high molecular flexibility for a high ionic conductivity, while the mechanical stability is provided by the hard segment. The hard segment is composed of urethane linkages (−NHCOO−) that contribute to the mechanical stability.[38] The mechanical strength originates from hydrogen bonding groups between C═O and N−H in different urethane chains, which physically cross-link the segments in the structure.[38,39] Several soft segment approaches have previously been studied in polyurethane combinations, for example, ether-based polyurethanes,[40] polycarbonate-based polyurethanes,[41] single-ion-polyurethane electrolytes,[42] and self-healing polyurethanes.[43]

The modular design principle of polyurethanes allows, at least in theory, for separately designing the soft and hard segments for ion conduction and mechanical robustness, respectively. The question is then how well these respective properties will be retained in the composite polyurethane electrolyte, which also incorporates an ionic component. In this study, the design of the soft segments in a series of polyurethane and their properties as host materials for SPEs for high-temperature lithium metal batteries have been investigated. The design aspect has been extended to not only include the mechanical and ion transport properties but also the solubility of the materials in volatile organic solvents to enable facile processing into solvent-free electrolyte films. The structural influence of the soft segment on the intrinsic ion transport properties and the mechanical stability of the polyurethanes have been investigated along with their temperature dependence. Ultimately, the electrochemical performance of the polyurethanes as SPEs in high-temperature batteries has been evaluated.

EXPERIMENTAL SECTION

Soft Segments. For use as polyester/polycarbonate soft blocks, 1000 g mol^{-1} and 2000 g mol^{-1} poly(CL-*co*-TMC) was synthesized through ring-opening polymerization of the monomers ε-caprolactone (CL, Perstorp; distilled under reduced pressure over CaH_2) and trimethylene carbonate (TMC, Richman Chemical) in a molar ratio of 4:1 with the initiator 1,3-propandiol (98%, Sigma-Aldrich) and the catalyst Stannous 2-ethylhexanoate (95%, Sigma-Aldrich).[17] In an argon-filled glovebox, the materials were added to a reactor before it was sealed and transferred out of the glovebox and polymerized in an oven for 72 h at 130 °C. During the first few hours, the reactor was shaken occasionally to ensure homogeneous mixing. After polymerization, the reactor was transferred back into an argon-filled glovebox and the polymer was collected.

For the pure polycarbonate soft blocks, ETERNACOL PH1000 and PH2000 polycarbonate diols (UBE Corporation) were used. These are carbonate linked copolymers prepared from a 1:1 molar mixture of 1,5-pentanediol and 1:1 hexanediol and their molecular weights are 1000 g mol^{-1} and 2000 g mol^{-1}, respectively, as determined from their hydroxyl numbers obtained by titration with potassium hydroxide.

Polyurethane Synthesis. The polyurethane compositions were prepared in cyclopentanone or tetrahydrofuran using the general procedure described below. Methylene di-p-phenyl diisocyanate (MDI, 98%), 2-methyl-1,3-propanediol (MPD, 99+%), dibutyltin dilaurate (95%), cyclopentanone (>99%), and tetrahydrofuran (THF, anhydrous, >99.9%) were obtained from Sigma-Aldrich and used as obtained. MDI was stored under refrigeration until use and was allowed to warm to room temperature before opening the container.

The polyurethane materials were prepared at 30 wt % in the chosen reaction solvent. The reaction solvent was charged into a 250-ml round-bottom flask fitted with a nitrogen inlet, overhead paddle-type stirrer, and a reflux condenser, after which MDI, polycarbonate diol or poly(CL-*co*-TMC) diol, and MPD were added under nitrogen cover and dissolved in the solvent by stirring at room temperature. 4 mol % excess MDI based on the combined moles of polymeric diol and MPD was utilized to compensate for side reactions with trace amounts of moisture in the reaction mixture. Once the reactants were in solution, dibutyltin dilaurate (50−100 ppm) was added to the mixture to catalyze the polymerization reaction. The polymerization was initiated at 50 wt % polymer solids and the contents were then diluted over the first few hours to 30 wt % as the viscosity of the mixture increased. The reaction was then allowed to proceed overnight while stirring under nitrogen cover at room temperature. Transparent, viscous polymer solutions were obtained in all instances. When cyclopentanone was used as the reaction solvent, an initial exotherm of 20−40 °C was usually observed after adding the catalyst. However, when THF was used as the reaction solvent, an exotherm did not occur after initiating the polymerization. Consequently, it was found advantageous to preheat the reactants to 40 °C before adding the organotin catalyst to obtain consistent high viscosity solutions.

For electrical and thermo-mechanical studies, the polyurethane compositions were prepared in cyclopentanone and then precipitated by rapid stirring into a large volume of 50:50 water/methanol. The precipitated polymer solids were allowed to rest in the solution for 48 h to extract cyclopentanone and low-molecular-weight residues. They were then vacuum-dried at 50 °C for at least 24 h. GPC analysis before and after precipitation consistently showed a single elution peak corresponding to high-molecular-weight polymer chains. The synthesized polyurethane structures were validated by ^{1}H NMR measurements at 25 °C on a JEOL ECZ 400S 400 MHz nuclear magnetic resonance (NMR) spectrometer (Figures S1−S4).

Polymer Electrolyte Preparation. Polyurethane electrolyte films were prepared by solution casting in polytetrafluoroethylene (PTFE) molds of the dissolved polymers and lithium bis-(trifluoromethylsulfonyl)imide (LiTFSI, Solvionic, vacuum-dried at 120 °C for 48 h) in tetrahydrofuran (THF, anhydrous, ≥99.9%, inhibitor-free, Sigma-Aldrich) followed by controlled evaporation of the solvent as described elsewhere.[19,44] The weight percentage of LiTFSI was varied between 0 and 30 wt % of the total weight of the prepared polymer films. The thickness of the final polymers was between 100−200 μm and is specified when relevant.

Polymer Electrolyte Characterization. The thermal properties of the electrolyte films were studied by differential scanning calorimetry (DSC) on a TA Instruments DSC Q2000. The samples were prepared in hermetically sealed aluminum pans in an argon-filled glovebox and measured by cooling at a rate of 5 °C min^{-1} to −80 °C and subsequently heated at 10 °C min^{-1} up to 150, 180, or 200 °C.

The mechanical properties were characterized by an oscillatory rheology on an Advanced Rheometer 2000 (TA Instruments) with an 8 mm stainless steel parallel plate geometry. A frequency sweep was performed at the temperatures 25, 40, 55, 70, and 85 °C from 0.01 to 10 Hz with a controlled strain of 0.5%. A temperature sweep was also performed between 25 and 120 °C with an increment of 2 °C

https://doi.org/10.1021/acsaem.1c02942
ACS Appl. Energy Mater. 2022, 5, 407−418

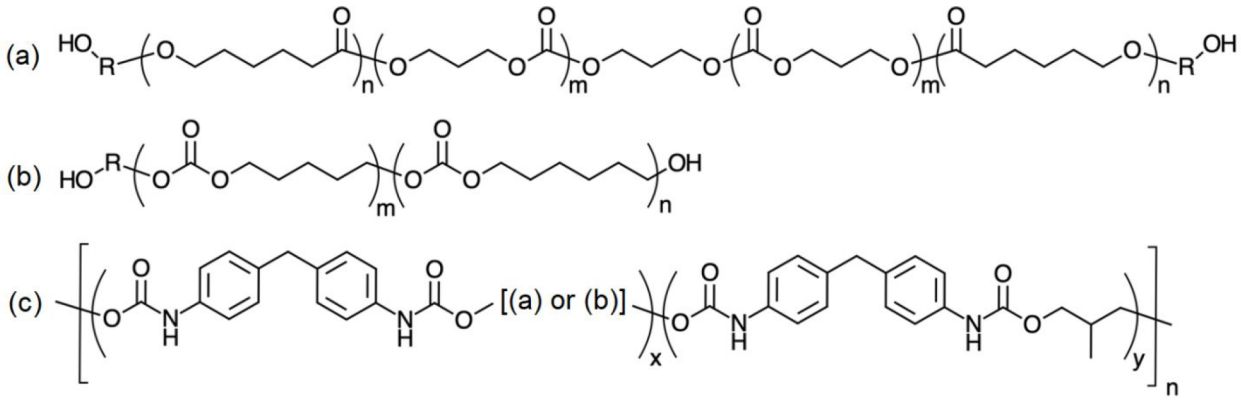

Figure 1. Structural depictions of (a) poly(CL-*co*-TMC), where m/n = 1:4 and R = caprolactyl or carboxypropyl radical, (b) polycarbonate, where $m = n$ and R = pentyl or hexyl radical, and (c) the generalized polyurethanes derived from them.

between each measurement at an angular frequency of 1 rad s^{-1} and a controlled strain of 0.5%. All measurements were carried out in a nitrogen atmosphere by covering the sample and geometry with a steel cover and a controlled normal force on the sample of 1 ± 0.1 N.

Electrochemical Characterization. The total ionic conductivity of the polymer electrolyte films was determined by electrochemical impedance spectroscopy (EIS) between the frequencies 1 Hz and 10 MHz at 10 mV amplitude with a Schlumberger SI 1260 Impedance/Gain-phase Analyzer. The electrolyte films were assembled with stainless steel blocking electrodes in CR2032 coin cells and annealed at 100 °C for 1 h and then cooled down to room temperature prior to the experiment to ensure good interfacial contact between the polymer and the stainless-steel electrodes. The measurements were carried out at temperature intervals of 10 °C between room temperature and 100 °C. The thickness was measured using a Mitutoyo digital indicator and is an average of four different measurements of each electrolyte film. The conductivity was calculated in ZView from the bulk resistance of the electrolyte film by fitting a Debye circuit to the impedance response.

The Li^+ transference number of the electrolyte films was determined by the Bruce–Vincent method[45] using a Bio-Logic SP-240 Potentiostat for the impedance spectroscopy and potentiostatic polarization measurements. The measurements were conducted at 80 °C with a symmetrical cell setup, where the electrolyte film was sandwiched between two lithium electrodes and assembled in a pouch cell. Prior to the measurement, the cell was allowed to equilibrate at the set temperature for at least 48 h or until a steady resistance was achieved. The impedance measurement was performed between 1 MHz and 100 mHz with an amplitude of 20 mV and a bias of 0 V and 10 mV before and after the polarization, respectively. The chronoamperometric polarization was conducted with an applied bias of 10 mV until a steady-state current was obtained. The electrolyte bulk resistance and interfacial resistance between the electrolyte and electrode was calculated in ZView and the initial current was determined by the approach developed by Hiller et al.[46]

The electrochemical stability of the electrolyte films was determined by linear sweep voltammetry (LSV). The measurements were performed at 80 °C with a scan rate of 0.1 mV s^{-1} by sweeping from open circuit voltage (OCV) to 6 V and back to 2.5 V. Five cycles were performed. The oxidation stability potential was studied with carbon-coated aluminum as the working electrode (WE) and lithium metal as the counter electrode (CE) in CR2032 coin cells.

Electrode Preparation. $LiFePO_4$ (LFP) (Phostech, P2 nano-sized) electrodes were prepared by ball milling the active material with carbon black (CB, C65, Imerys) and the polymer electrolyte as a binder (varied to be the same as the electrolyte between the electrodes) with the ratio LFP/CB/binder = 70:15:15 in THF. The electrode slurry was coated on carbon-coated aluminum foil with a doctor blade gap of 150 μm. The electrode was thereafter allowed to dry in ambient temperature for at least 24 h, before finally dried in a vacuum oven at 120 °C for 12 h. The diameter of the electrodes was 12 mm with an active mass loading of 1.8–2.4 mg cm^{-2}.

Battery Cycling. Type CR2032 coin cells were assembled from electrode–SPE assemblies prepared by casting the polymer electrolyte solution on top of LFP working electrodes, using the same procedure as described under Polymer electrolyte preparation, with Li metal as the counter electrode. To ensure good interfacial contact between the materials, the cells were allowed to rest for 24 h at 80 °C. Galvanostatic cycling tests of the electrolyte films were performed with an ARBIN BT-2043 cycling equipment at 80 °C.

RESULTS AND DISCUSSION

The key to designing polyurethane SPEs with high ionic conductivity is to understand the influence of the soft segment and how it is affecting the transport properties. Normally, a low molecular weight of the ion-conducting polymer is preferred to achieve high ionic conductivity since that will facilitate the chain dynamics. At molecular weights under 2000 g mol^{-1}, vehicular transport becomes the dominating ion transport mechanism, in contrast with the segmental motion-assisted ion transport at higher molecular weights.[17,27,47,48] Part of the increased dynamics at low molecular weights originates from the freely moving chain ends. In polyurethanes, however, the chain ends of the soft ion-conducting segments are covalently bonded in the structure to the hard segment. This will restrict the segmental dynamics of the chains and thereby limit the ionic conductivity. The proportion of the soft segment in the structure of the polyurethane will also influence the ionic conductivity, considering that a larger amount of the soft segment allows for more pathways for ion conduction in the polymer matrix. The choice of soft segment is another factor to consider when designing the polyurethane, as it has been seen that the strength of the interaction between the coordinating groups on the polymer and the cations in the system directly affects the ionic conductivity and transference number (T_+), which together describe the ion transport abilities in the system.[17] Considering this, soft blocks based on polycarbonates and polyesters were targeted for the polyurethane preparation, as these classes of materials have shown weak ion coordination leading to high T_+ and improved battery performance compared to poly(ethylene oxide) (PEO), which is otherwise the most widely studied host materials for SPEs.[49,50] In particular, the copolymer between ε-caprolactone and trimethylene carbonate (poly(CL-*co*-TMC)) with an amorphous morphology and low T_g has demonstrated promising qualities in this regard.[44] The poly(CL-*co*-TMC), which consists of ion-coordinating carbonyl groups from the

https://doi.org/10.1021/acsaem.1c02942
ACS Appl. Energy Mater. 2022, 5, 407–418

Table 1. Molecular Weight and Soft Segment Content of the Polyurethanes Studied

polyurethane	soft segment polymer	soft segment M_n/g mol^{-1}	soft segment content/wt %	total M_n/g mol^{-1}	PDI[a]
BPP1000	poly(CL-*co*-TMC)	1000	74.2	59 700	2.05
BPP2000	poly(CL-*co*-TMC)	2000	67.3	65 300	2.05
PH1000	polycarbonate diol	1000	74.2	47 800	1.79
PH2000	polycarbonate diol	2000	67.3	41 172	1.91

[a]Polydispersity index.

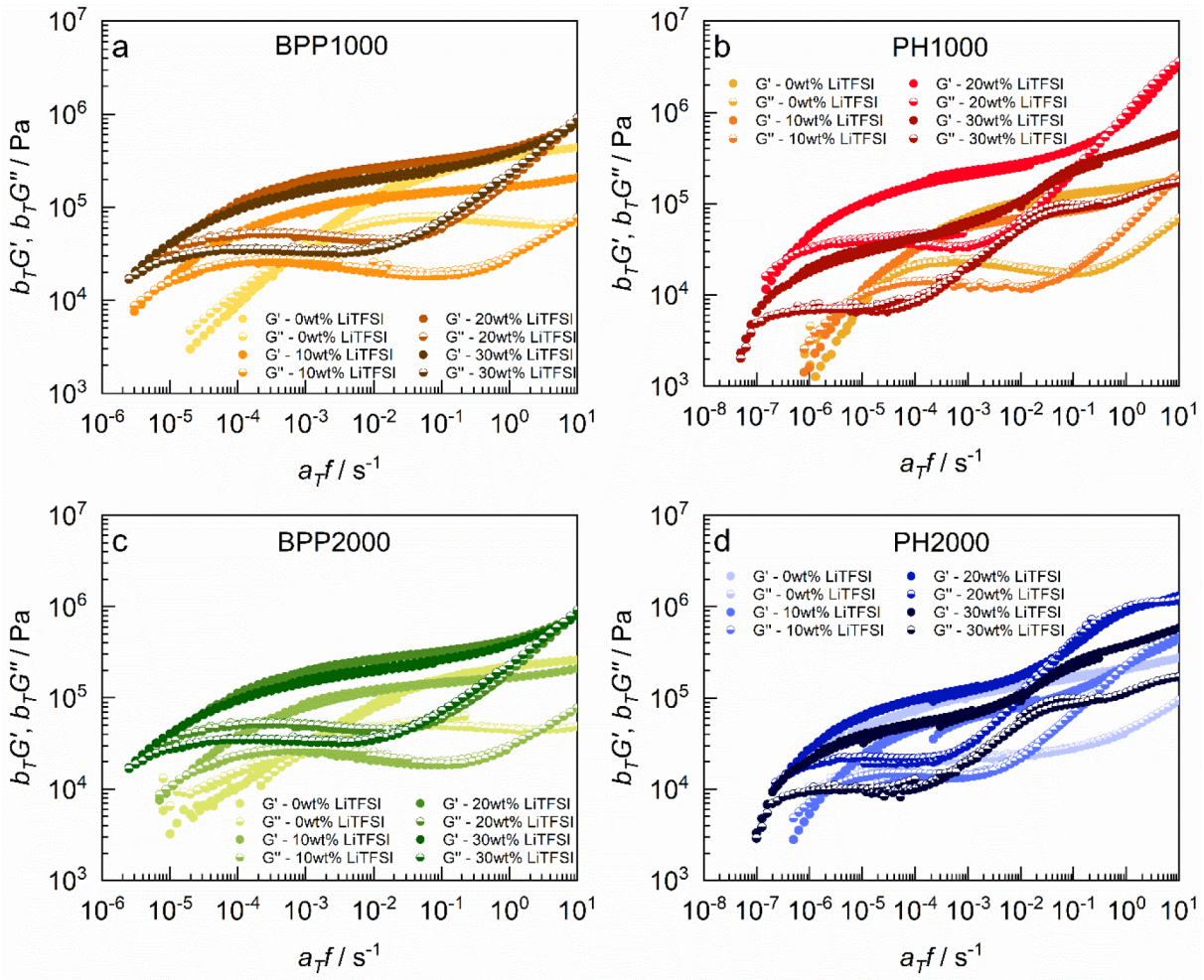

Figure 2. Time−temperature superposition master curves of the polyurethanes with 0−30 wt % LiTFSI with 25 °C as the reference temperature.

carboxylate and carbonate ester units in the chain, was used along with a second soft block based on a polycarbonate diol comprising carbonyl groups only originating from carbonate esters.

Another important design consideration is processability. Designing the polyurethanes to be soluble in THF instead of the more commonly used casting solvents such as dimethylformamide (DMF), dimethyl sulfoxide (DMSO), and *n*-methyl-2-pyrrolidone (NMP) enables easier processability and removal of solvent residues during manufacturing, due to the more volatile nature of THF.[13] Polyurethanes with high hard segment contents (>40% of polymer mass) are often soluble only in strong polar aprotic solvents like NMP. Likewise, solubility also becomes more restricted at polymeric diol molecular weights below 1000 g mol^{-1}. As a result, polymeric diols with higher molecular weight was used, and the hard segment content was confined to less than 35% of the polymer mass. A branched chain extender (MPD) was selected to introduce disorder into the hard segments and reduce interchain hydrogen bonding. The chemical structures of the polymeric soft block segments and a generalized structure for the polyurethanes derived from them can be seen in Figure 1.

When performing the polyurethane synthesis with all of the design criteria in mind, it was found that when utilizing polymeric diols with molecular weights of 1000 g mol^{-1}, polyurethanes with consistently high molecular weights could be obtained for a soft segment content as high as ∼75% of the total polymer mass. On the other hand, when utilizing polymeric diols with molecular weights of 2000 g mol^{-1}, the polyurethane molecular weights were inconsistent and generally lower when the soft segment content was greater than about 65% of total polymer mass. One explanation for this might be the longer hard segments formed when the soft segments have higher molecular weight, leading to poorer

https://doi.org/10.1021/acsaem.1c02942
ACS Appl. Energy Mater. 2022, 5, 407−418

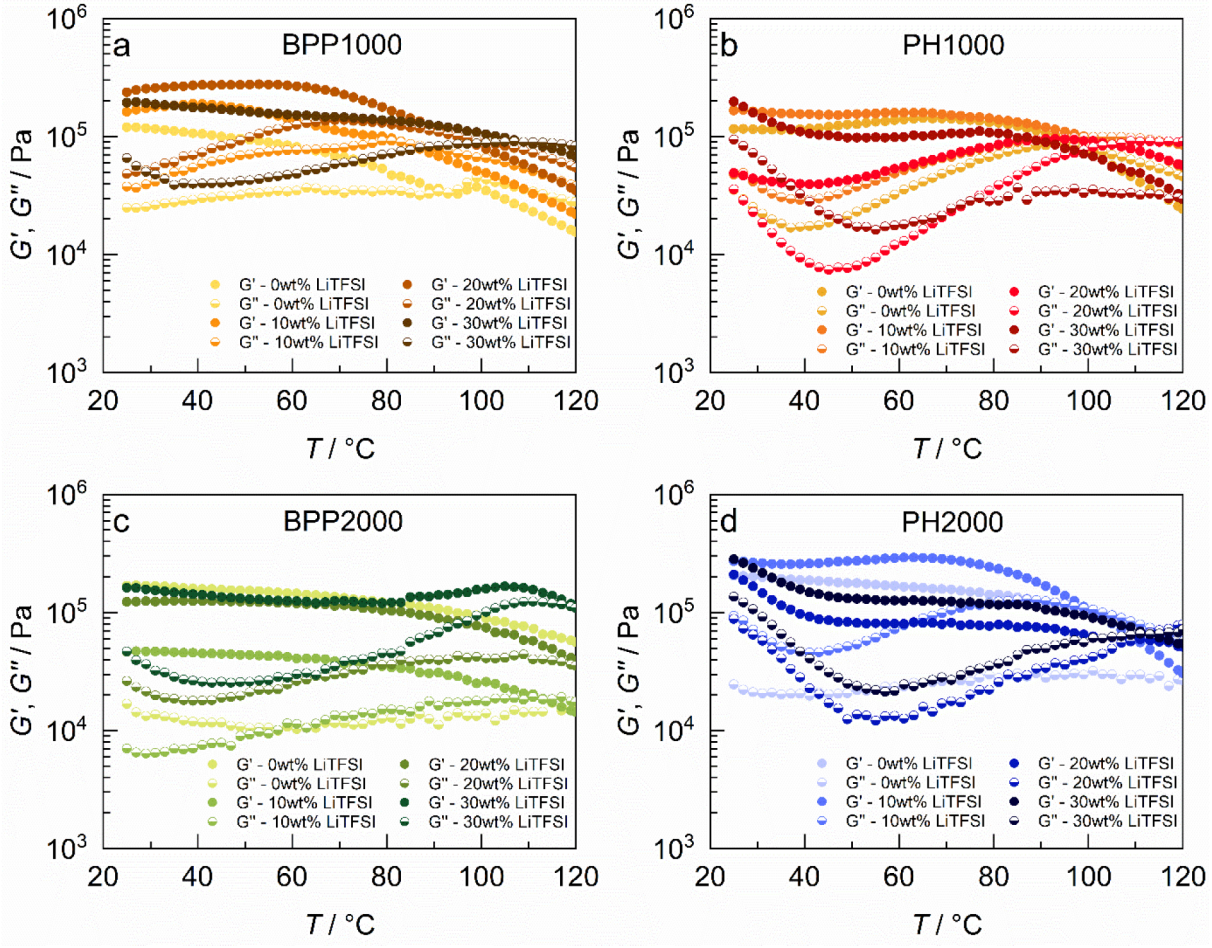

Figure 3. Temperature sweep of the polyurethanes with salt concentrations between 0−30 wt % based on the total weight of the polyurethane.

solubility and inconsistent total molecular weights of the final product. No obvious solubility issues were observed during the synthesis, however, and the lower molecular weights may instead be an effect of the reaction kinetics due to the slower dynamics and diffusion of the longer soft segments. As a result, the molar proportions of MDI-to-polymeric diol-to-MPD were fixed at 100:80:20 when using the lower-molecular-weight (1000 g mol^{-1}) soft segment components, which corresponded to 74.2 wt % polymeric diol in the final polyurethane product. When using the higher-molecular-weight (2000 g mol^{-1}) soft segment components, the molar proportions were fixed at 100:33:67, which corresponded to 67.3 wt % polymeric diol in the polyurethane product.

The compositions and molecular weights of the investigated polyurethanes are shown in Table 1. All products featured a high average molecular weight and showed complete solubility in THF, with no turbidity or gelatinous properties present in solutions containing as much as 30 wt % polymer solids. Throughout the text, the mentioned salt contents are based on the total weight of the polyurethanes unless otherwise stated. Specific compositions are abbreviated equivalent to BPP2000-20, where the part before the dash indicates the type of polyurethane and the molecular weight of the soft segment, while the number after the dash indicates the salt concentration based on the total weight.

In sharp contrast to the essentially liquid low-molecular-weight diols used as the starting material for the polyurethane synthesis, all prepared polyurethanes were tough and nonsticky both in their pure form and when combined with LiTFSI salt, which made them easy to handle and process, suggesting high mechanical stability necessary for high-temperature use. Digital photos of a synthesized polyurethane and a solution-cast polyurethane film with salt are shown in Figure S5.

To study the mechanical stability of the aforementioned polyurethanes, two types of rheological measurements of the storage (G') and loss modulus (G'') were performed; first a wide frequency range measurement and specifically at very low frequencies (long time scales) and second a wide temperature range measurement were conducted. The stability at low frequencies is interesting since it mimics the static stresses the electrolyte membrane is exposed to under pressure in a battery cell during ordinary cycling conditions. To access information at extremely low frequencies of deformation, the time−temperature superposition (TTS) principle was applied to construct a master curve spanning several orders of magnitude of frequencies within an acceptable time frame.[51] In Figure 2, TTS superposition master curves for the polyurethanes with 0−30 wt % LiTFSI constructed from the frequency sweep measurements are shown, with the reference temperature set at 25 °C. All materials show considerable mechanical stability, with the crossover of G' and G'' (indicating a transition from solid-like to liquid-like behavior) located below 10^{-2} Hz for the BPP-polyurethanes and even below 10^{-4} Hz for the PH-polyurethanes. Similar to what is observed for pure high-molecular-weight poly(CL-*co*-TMC),[52] the static mechanical stability increases when LiTFSI salt is added, seen as a shift of

https://doi.org/10.1021/acsaem.1c02942
ACS Appl. Energy Mater. 2022, 5, 407−418

the crossover to lower oscillation frequencies (i.e., longer time scales). This is an effect arising from the transient physical cross-links formed from the interaction between the polymer chains and the Li^+ ions at higher LiTFSI concentrations.[13,19,53] While there is no obvious and consistent difference in mechanical response between the different molecular weights of the soft block, there is a distinct difference between the BPP- and PH-polyurethanes with the latter consistently showing mechanical stability extended to lower frequencies, indicating an overall better mechanical stability regardless of salt concentration.

The temperature dependence of the mechanical response was evaluated by temperature sweeps of the polyurethanes with 0−30 wt % LiTFSI between 25−120 °C (Figure 3) to investigate the upper temperature limit for the polyurethanes and where the materials start to flow. Initially, the addition of LiTFSI is seen to have a negative impact on the mechanical stability at elevated temperatures for all of the materials, as the crossover between the storage and loss modulus is shifted to lower temperatures for all polyurethanes when 10 wt % LiTFSI is added. This indicates that the addition of salt weakens the intermolecular interactions that are largely responsible for the mechanical stability of the materials, that is, the hydrogen bonding between the urethane groups of the hard blocks.[54] However, when the LiTFSI concentration is increased further beyond 10 wt % LiTFSI, the limit to mechanical stability is pushed toward higher temperatures, which can be explained by cross-linking effects arising at higher salt concentrations.[13,19,53] For both polyurethanes, there appears to be a trend that the materials with a high molecular weight of the soft segments (2000 g mol^{-1}) demonstrate a greater mechanical stability at elevated temperatures for all LiTFSI concentrations despite exhibiting similar response in the frequency sweep measurements (Figure 2) as the polyurethanes with 1000 g mol^{-1} soft segments. BPP1000 was found to be the most temperature-sensitive polyurethane, where the only composition mechanically stable above 100 °C was with 30 wt % LiTFSI. In contrast, BPP2000 displays superior mechanical stability up to 110 °C for all salt concentrations with PH1000 and PH2000 falling in between. A higher molecular weight of the soft block should lead to a softer material, as the longer chains between the "locking points" of the hard blocks will have more flexibility. At the same time, the longer soft segments will have more opportunities for cationic cross-linking and entanglements in the structure.[55,56] In this case, the observed effect is likely to also be influenced by the higher proportion of hard segments present in the 2000 g mol^{-1} polyurethanes, originating from the hard and rigid urethane groups in the structure that stiffens the structure. In addition, the hard segments are longer for the 2000 g mol^{-1} polyurethanes (972 g mol^{-1} vs 348 g mol^{-1}, estimated from the proportions of hard and soft segments and assuming a 1:1 stoichiometric ratio), which is likely to have large influence on the mechanical properties.

The T_g was determined for the polyurethanes to gain insight into the flexibility of the polymer chains, which gives an indication of how well the cation can be transported by the segmental motion of the polymer.[57] In Figure 4, the influence of the LiTFSI content based on the total polyurethane weight on the T_g of the polyurethanes is shown. As expected, the T_g of the polyurethanes is increasing with increasing LiTFSI content as the guest cations have an ionic cross-linking effect on the polyurethane chains.[13,19,53] These findings are in accordance

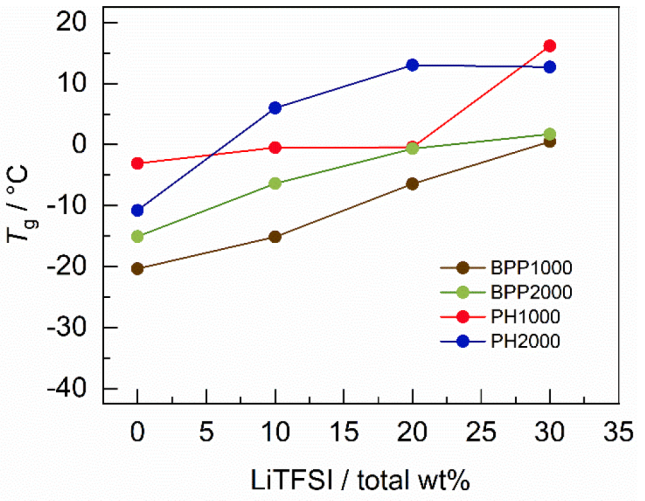

Figure 4. T_g of the polyurethanes at different salt concentrations. The salt concentrations are based on the total weight of the polymers.

with the increased mechanical stability with increasing salt content stemming from the cross-linking network. From these results, it is also clear that the poly(CL-*co*-TMC)-based polyurethanes have a distinctly lower T_g than the polycarbonate diol-based compositions for all LiTFSI concentrations, suggesting a higher chain flexibility in the former. This translates into faster chain dynamics of the poly(CL-*co*-TMC) soft segments, which will ultimately affect the rate of ionic transport in the polyurethane. Comparing the T_g of the poly(CL-*co*-TMC) polyurethane containing 27−30 wt % LiTFSI based on the soft segment weight (Figures S6 and S7) with pure high-molecular-weight poly(CL-*co*-TMC) containing 28 wt % LiTFSI (poly(CL-*co*-TMC)-28), apparent differences are observed. While a T_g between −6 and 0 °C is observed for both BPP1000-20 and BPP2000-20, the high-molecular-weight poly(CL-*co*-TMC)-28 exhibits a T_g of −37 °C. This apparent difference originates from the locked chain ends of the soft segments in the polyurethane structure, which slows down the total segmental dynamics of the polymer chains compared to in the high-molecular-weight poly(CL-*co*-TMC)-28. In the latter, the length of the flexible segments is instead limited by chain entanglements together with ion−polymer interactions, which both constitute transient physical locking points. This constitutes a significant penalty to the chain flexibility and ultimately also the ability of the polymer hosts to support fast ion transport at lower temperatures. This renders the polyurethane SPEs useful solely for applications operating above room temperature, where the chain dynamics may be sufficiently fast. However, as noted by the mechanical stability measurements, the polyurethanes show robust mechanical properties up above 100 °C depending on the design of the material, making high-temperature application an attractive option.

While the T_g is found to be lower for the polyurethanes based on the low-molecular-weight diols, this is likely not a direct effect of the molecular weight of the soft segments, as the restriction of the chain ends imposed by incorporating the diols into the polyurethane chains significantly increases the T_g. For comparison, the T_g for the poly(CL-*co*-TMC) diols was determined to be −68 °C and −62 °C for the 1000 g mol^{-1} and 2000 g mol^{-1} diol, respectively. In contrast to the soft segments of the polyurethanes, the segmental mobility of the

https://doi.org/10.1021/acsaem.1c02942
ACS Appl. Energy Mater. 2022, 5, 407−418

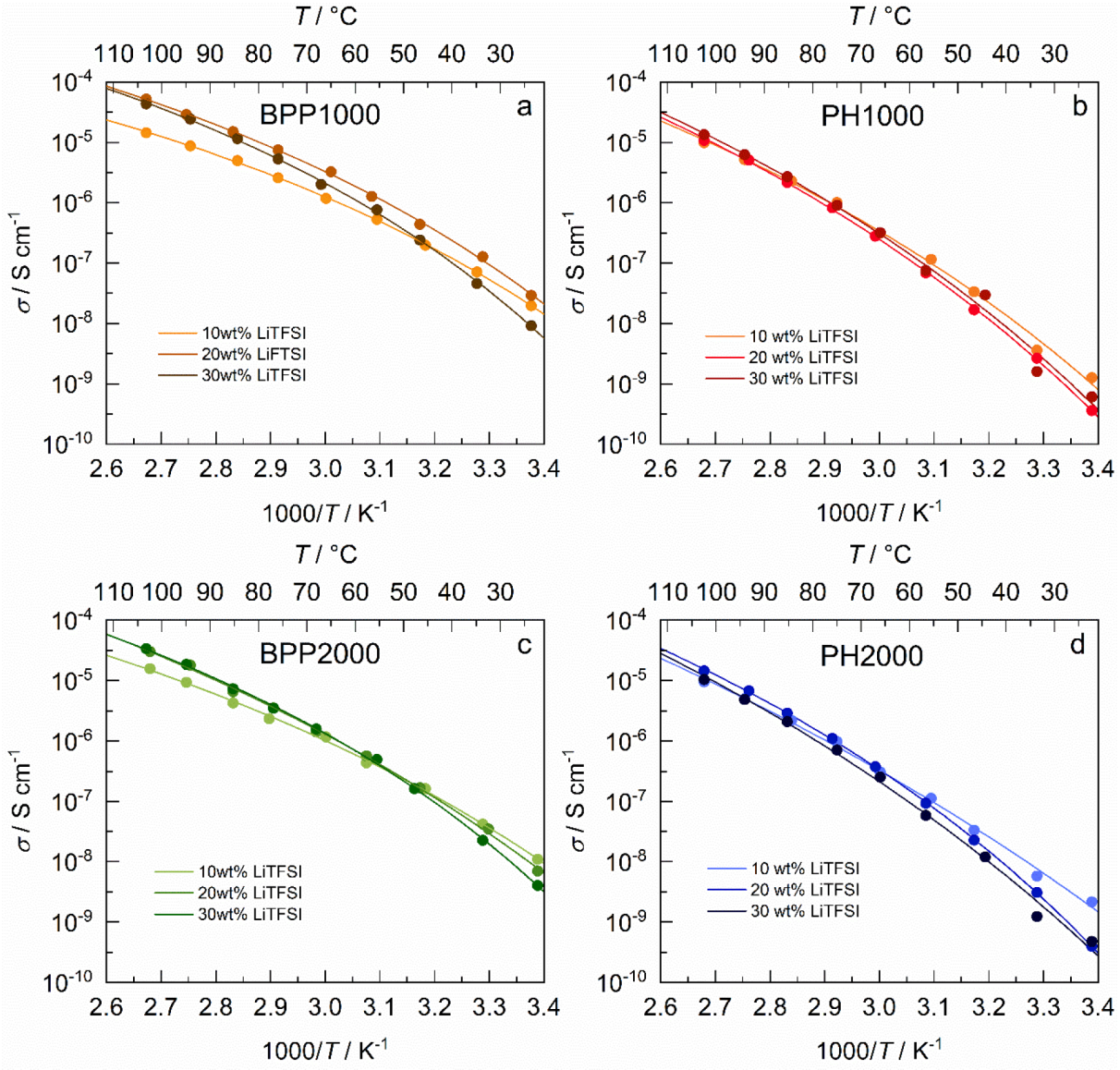

Figure 5. Ionic conductivity of the polyurethanes at different salt concentrations based on the total weight of the polymer.

diols is heavily influenced by the end-groups and the T_g is poorly representative of the T_g of the resulting polyurethanes. The lower T_g of the low-molecular-weight polyurethanes is thus likely to instead originate from the higher proportion of soft segments in the structure, although it should also be acknowledged that phase mixing can also have a large influence on the T_g for polyurethanes.

The effect of T_g on conductivity can be seen in Figure 5, showing the ionic conductivity of the polyurethanes, where the differences in T_g are reflected in the ionic conductivity of the polyurethanes, with the poly(CL-*co*-TMC)-based polyurethanes in general showing higher ionic conductivity than the polycarbonate diol polyurethanes. The temperature dependence of the ionic conductivity follows a Vogel–Fulcher–Tamman (VFT) behavior,[58−60] indicating that the ion transport characteristics are retained when incorporating segments into the polyurethane structure with the Li^+ transport being coupled to the segmental motions of the soft block. The higher ionic conductivity for the poly(CL-*co*-TMC)-based polyurethanes thus originates in the higher molecular flexibility and faster chain dynamics of this polymer, as indicated by the lower T_g. The highest ionic conductivity was obtained for the higher salt concentrations of 20 and 30 wt % LiTFSI at high temperatures. The highest ionic conductivity is observed for BPP1000 with a maximum of 0.052 mS cm^{-1} at 100 °C compared to 0.030 mS cm^{-1} for BPP2000 at 100 °C, which is in accordance with the lower T_g for BPP1000. The polycarbonate diol samples displayed similar ionic conductivity to each other at all temperatures and LiTFSI concentrations with a maximum of 0.014 mS cm^{-1} for PH1000 at 100 °C.

Comparing the results of the polyurethanes with the high-molecular-weight poly(CL-*co*-TMC)-28 with a similar salt content[49] (Figure 6), it is clear that ionic motion is impaired when the poly(CL-*co*-TMC) is incorporated in the polyurethane, as the ionic conductivity decreases by 1 order of magnitude or more and the T_g is increased by more than 40 °C (Figure S7). The low ionic conductivity for the polyurethanes compared to the poly(CL-*co*-TMC)-28 can partly be explained by the locked chain ends of the short ionically conducting soft segments in the polyurethanes, as evidenced by the increased T_g values. In addition, since the polyurethanes also consist of both soft and hard segments, where only the soft segments are

https://doi.org/10.1021/acsaem.1c02942
ACS Appl. Energy Mater. 2022, 5, 407−418

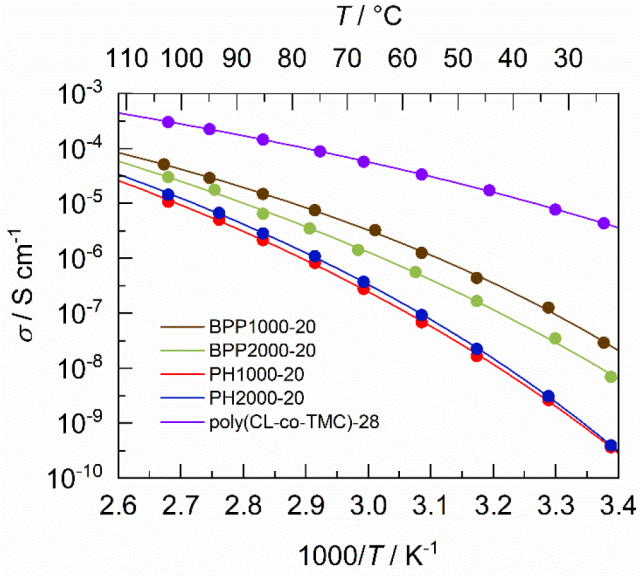

Figure 6. Ionic conductivity of the polyurethanes with 27−30 wt % LiTFSI (based on the weight of the soft segments in the polyurethanes) and pure high-molecular-weight poly(CL-*co*-TMC) with 28 wt % LiTFSI. Please note that the notations of salt content in the figure are based on the total weight of the polyurethanes.

ion-conducting, the pathways through the polymer are restricted to the part of the matrix formed by the soft segments. This limits the freedom of movement of the Li^+ ion and consequently reduces the ionic conductivity. Lastly, the larger proportion of nonconducting content from the hard mechanically stable urethane segments in the polyurethanes is contributing to the lower ionic conductivity, as less material can contribute to the Li^+ ion transport. However, at elevated temperatures the fast chain dynamics of the poly(CL-*co*-TMC)-28 result in insufficient mechanical stabilization from entanglements alone, causing the material to quickly reach its mechanical stability limit.[21,52] As demonstrated here, this can be improved by incorporating it into a polyurethane chain, rendering this promising SPE platform also useful at high temperatures.

The cation transference number (T_+) of the polyurethane electrolytes was measured at 80 °C using the Bruce−Vincent method.[45] The results of the impedance measurements before and after the polarization, the current during polarization, and the equivalent circuit used to determine the resistances are shown in Figures S8 and S9. From these measurements, the transference number was calculated by

$$T_+ = \frac{I_{SS}(\Delta V - I_0 R_{int,0})}{I_0(\Delta V - I_{SS} R_{int,SS})} \quad (1)$$

where I_0 and I_{SS} are the initial and steady state current respectively (before and after polarization), the $R_{int,0}$ and $R_{int,SS}$ are the interface resistances initially and at steady state current and ΔV is the applied bias voltage. I_0 was calculated from the bulk resistance of the electrolyte according to the method proposed by Hiller et al.[46] The calculated transference numbers from the measurement are shown in Table 2. All polyurethanes display a transference number around 0.6. This is very similar to the T_+ value of 0.66 reported for high-molecular-weight poly(CL-*co*-TMC) at a similar salt concentration.[61] This confirms that the conduction mechanism in the

Table 2. Calculated Transference Number for Each Polyurethane with a Salt Concentration of 20 wt % Based on the Total Weight of the Polyurethanes

polyurethane	T_+
BPP1000-20	0.61
BPP2000-20	0.63
PH1000-20	0.67
PH2000-20	0.56

poly(CL-*co*-TMC) is retained when incorporated as the soft segment in the polyurethanes. The Li^+ ions are thus mainly transported in the soft segment in the structure and the hard urethane segments are merely contributing to the mechanical stability.

As recently reported by Rosenwinkel et al., the cation transference number is determined by the coordination strength of the Li^+ cations to the polymer chains.[17] Previous studies have shown higher T_+ for electrolytes based on the polycarbonate poly(trimethylene carbonate) than for electrolytes based on the poly(CL-*co*-TMC) copolymer.[17,61] In contrast, very similar T_+ values are seen here for the polyurethane systems. This indicates that, while poly(trimethylene carbonate) has a weak affinity for Li^+, the polycarbonate soft segments used for the PH-polyurethanes are more similar to poly(CL-*co*-TMC) in its ion coordination properties. This implies that the ion coordination properties of these polymers are not only affected by the coordinating functional groups but by the overall structure of the coordinating polymer as well. The longer aliphatic carbon chains in the PH-polyurethanes compared to poly(trimethylene carbonate) seem to enhance the affinity of the carbonate group to Li^+, yielding a reduced T_+.

The signs of preserved conduction mechanism of Li^+-ions when incorporating a polymer chain as the soft segment in polyurethanes enlighten the power of utilizing polyurethanes as a SPE for lithium metal batteries. Considering that the ion conduction mechanism remains the same for the soft segment in the polyurethane as for the pure polymer, it is possible to design the polyurethane to achieve desirable properties for utilization as an SPE in lithium metal batteries by controlling the hard and soft segments ratios and by the choice of polymer type and molecular weight of the soft segments as the ionically conducting part. As the ion transport characteristics are carried over from the soft block to the polyurethane electrolytes, this means that soft blocks with low T_g combined with weak interactions with Li^+ are optimal to design polyurethanes with fast Li^+ conduction while potentially retaining mechanical integrity at elevated temperatures.

On the basis of this evaluation, BPP2000-20 was selected for further evaluation of the electrochemical properties, since the poly(CL-*co*-TMC) polyurethanes exhibited superior properties compared to the polycarbonate diol polyurethanes and the BPP2000 displayed the highest mechanical stability of the studied polyurethanes and an ionic conductivity of the same order of magnitude as BPP1000.

The electrochemical stability at high potentials was studied through cyclic voltammetry (CV) measurements of the BPP2000−20 electrolyte (Figure 7) at 80 °C. Five consecutive scans were conducted. On the first scan, we observe an oxidation current onset at ∼3.5 V vs Li^+/Li which is interpreted as electrolyte oxidation, which has previously been observed for polycarbonates at 3.5 V.[62] However, with

https://doi.org/10.1021/acsaem.1c02942
ACS Appl. Energy Mater. 2022, 5, 407−418

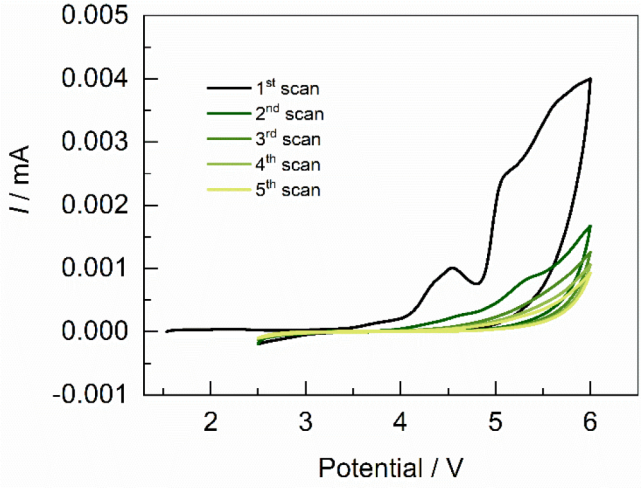

Figure 7. CV measurement of BPP2000−20 performed with a scan rate of 0.1 mV s^{-1} at 80 °C.

increasing number of scans, the onset of the oxidation current is increased up to 4.5 V vs Li^+/Li in the fifth scan. This is an indication that the irreversibly formed species on the surface of the working electrode protect the SPE from further degradation on consecutive scans, that is, a passivation layer on the working electrode is formed.[63,64] During consecutive scans, the formed passivation layer aids the electrolyte to withstand higher potentials and will ultimately extend its lifetime and cyclability.

Long-term galvanostatic cycling of BPP2000−20 in cells consisting of LFP cathodes and lithium metal as the anode were performed at charge/discharge rates of C/10 and C/5 at 80 °C (Figure 8). Initially, issues were faced during the construction of the cells with many failed cycling attempts. The issues appeared to originate from insufficient infiltration of the SPE into the porous LFP electrode, leading to a large portion of the LFP being inaccessible for Li^+ transport, ultimately failing the cells. Because of the high mechanical stability of the electrolytes, even at high temperatures, there is insufficient flow of the material into the pores of the cathode to form ionic pathways and a well-connected electrolyte−electrode interface throughout the porous cathode. Part of the problem could be eased by increasing the temperature for the cycling and thereby facilitating better infiltration of the cathode with the SPE. Still, the resistance was too large to obtain decent cycling performance. However, by incorporating the BPP2000 polyurethane into the LFP electrode as the binder and solution casting the BPP2000-20 on top of the LFP electrode, an immense improvement in cycling performance was obtained. Further improvement was attained by lowering the upper cutoff potential (without losing capacity) which reduces the risk of uncontrolled electrolyte degradation. The final improvement was achieved when precycling the cells at C/40 for two conditioning cycles to ensure proper infiltration of the SPE in the LFP electrode and establishing stable and uniform solid/cathode electrolyte interphase (SEI/CEI) layers on each electrode surface and ensuring good adhesion between the electrodes and the electrolyte for continued cycling (Figure S10). After a few unsteady initial cycles, stable and continuous cycling was eventually obtained (Figure S11). The cell containing BPP2000-20 cycled at C/10 demonstrates an initial discharge capacity of 163 mAh g^{-1} in the first cycle after the

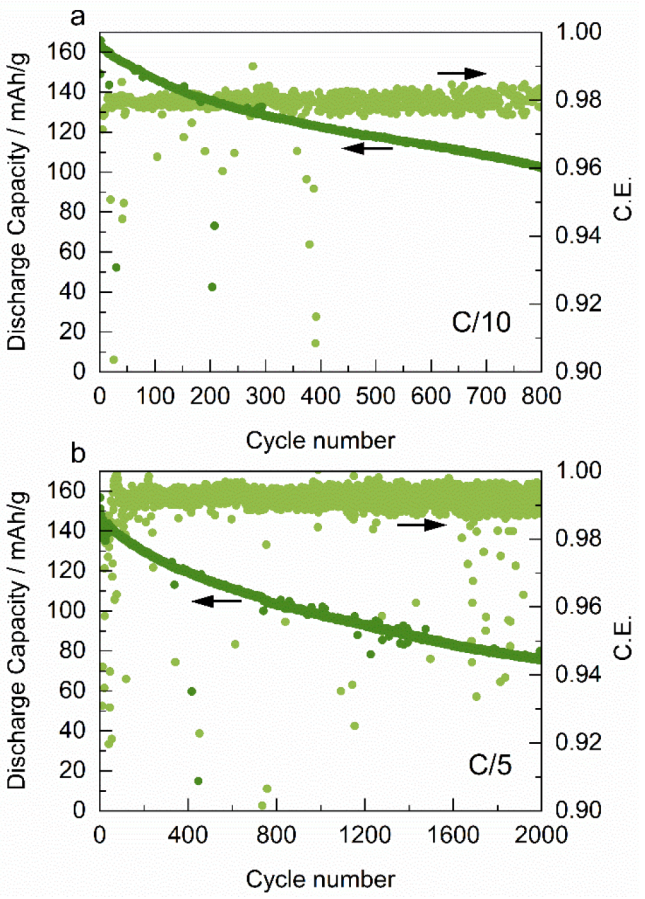

Figure 8. Cycling of LFP|BPP2000−20|Li cells at a rate of (a) C/10 and (b) C/5 at 80 °C.

initial conditioning cycles and 100 mAh g^{-1} after 800 cycles (capacity retention of 61%). When cycling the cell containing BPP2000-20 at C/5, a slightly lower initial capacity of 151 mAh g^{-1} was observed but still showing stable long-term cycling stability after 2000 cycles with a capacity of 76 mAh g^{-1}. The evolution of the voltage profile during cycling of BPP2000-20 at C/5 (Figure S12) supports the theory of a formed passivation layer, showing a polarization resistance already at the beginning of cycling. During the consecutive ~2000 cycles, only a slight increase of the polarization resistance in the cell is observed, indicating the formed passivation layer protects the SPE from further degradation at high temperatures.

Regarding the C.E., some minor fluctuations between 0.9−1.0 can be seen. However, considering the amount of cycles (2000 for the cell cycled at C/5), in addition to that the cells always recover the capacity after the lower-C.E. cycles, these fluctuations appear not to be the result of irreversible damage to either the electrodes or the electrolyte. The cycling results confirm the mechanical robustness of the polyurethanes and illustrates how the mechanical stability of the BPP2000-20 electrolyte can support long-term cycling at 80 °C, with reliable performance observed after one year of continuous cycling of the cells. At the same time, the long-term electrochemical stability toward metallic lithium and LFP at 80 °C is clearly sufficient to sustain extended cycling under these conditions.

https://doi.org/10.1021/acsaem.1c02942
ACS Appl. Energy Mater. 2022, 5, 407−418

CONCLUSIONS

The properties of polyurethanes with either poly(CL-*co*-TMC) or a polycarbonate diol as the soft segment have been investigated for application as SPEs in high-temperature lithium metal batteries. The studied polyurethanes show high stability toward flow at low rates of deformation and mechanical stability at temperatures up to and above 100 °C, demonstrating the strength supplied by the hard urethane segments. Observations also illustrate that the mechanical properties of the polyurethanes can be tuned by the properties of the soft segment. Considering the ion transport properties, the results indicate transferrable abilities from the pure polymer to the polyurethanes when incorporated as the soft segment, allowing for designing the polyurethanes host material for a combination of mechanical strength, fast ion transport, and processability by adjusting the segment ratios and by tailoring the structure of the soft segment. However, compared to a high-molecular-weight analog of the soft segment by itself, a distinct reduction of the ionic conductivity is observed. The reduced ionic conductivity originates from the locked chain ends of the soft segment by the hard segments, limiting the flexibility and segmental dynamics of the soft segments.

Electrochemical measurements confirm the long-term function of the poly(CL-*co*-TMC) polyurethane at high temperatures in a lithium metal battery, still cycling after 2000 cycles at 80 °C. Although possessing limited ionic conductivity, polyurethanes have thereby proven to be mechanically robust enough at high temperatures and to be compatible with the Li metal cell setup. This is an attractive set of features and, considering the design possibility of the polyurethanes, there is a future potential for utilization of polyurethane SPEs with appropriately designed structure and composition.

ASSOCIATED CONTENT

Supporting Information

The Supporting Information is available free of charge at https://pubs.acs.org/doi/10.1021/acsaem.1c02942.

NMR spectra of polyurethanes; digital photos of as-synthesized BPP2000 and solution-cast BPP2000-20 polymer film; T_g data; DSC data for poly(CL-*co*-TMC); transference number data; voltage profiles from battery cycling (PDF)

AUTHOR INFORMATION

Corresponding Author

Jonas Mindemark − *Department of Chemistry − Ångström Laboratory, Uppsala University, SE-751 21 Uppsala, Sweden;* orcid.org/0000-0002-9862-7375; Email: jonas.mindemark@kemi.uu.se

Authors

Rassmus Andersson − *Department of Chemistry − Ångström Laboratory, Uppsala University, SE-751 21 Uppsala, Sweden;* orcid.org/0000-0002-0879-7603

Guiomar Hernández − *Department of Chemistry − Ångström Laboratory, Uppsala University, SE-751 21 Uppsala, Sweden;* orcid.org/0000-0002-2004-5869

Jennifer See − *Brewer Science, Rolla, Missouri 65401, United States*

Tony D. Flaim − *Brewer Science, Rolla, Missouri 65401, United States*

Daniel Brandell − *Department of Chemistry − Ångström Laboratory, Uppsala University, SE-751 21 Uppsala, Sweden;* orcid.org/0000-0002-8019-2801

Complete contact information is available at: https://pubs.acs.org/10.1021/acsaem.1c02942

Author Contributions

The manuscript was written through contributions of all authors. All authors have given approval to the final version of the manuscript.

Notes

The authors declare no competing financial interest.

ACKNOWLEDGMENTS

The authors acknowledge financial support from STandUP for Energy.

REFERENCES

(1) Alipour, M.; Ziebert, C.; Conte, F. V.; Kizilel, R. A Review on Temperature-Dependent Electrochemical Properties, Aging, and Performance of Lithium-Ion Cells. *Batteries* **2020**, *6* (3), 35.

(2) Wright, D. R.; Garcia-Araez, N.; Owen, J. R. Review on high temperature secondary Li-ion batteries. *Energy Procedia* **2018**, *151*, 174−181.

(3) Lin, X.; Salari, M.; Arava, L. M.; Ajayan, P. M.; Grinstaff, M. W. High temperature electrical energy storage: advances, challenges, and frontiers. *Chem. Soc. Rev.* **2016**, *45* (21), 5848−5887.

(4) Chen, D.; Jiang, J.; Kim, G.-H.; Yang, C.; Pesaran, A. Comparison of different cooling methods for lithium ion battery cells. *Appl. Therm. Eng.* **2016**, *94*, 846−854.

(5) Nitta, N.; Wu, F.; Lee, J. T.; Yushin, G. Li-ion battery materials: present and future. *Mater. Today* **2015**, *18* (5), 252−264.

(6) Tarascon, J. M.; Armand, M. Issues and challenges facing rechargeable lithium batteries. *Nature* **2001**, *414* (6861), 359−67.

(7) Zhang, X.-Q.; Zhao, C.-Z.; Huang, J.-Q.; Zhang, Q. Recent Advances in Energy Chemical Engineering of Next-Generation Lithium Batteries. *Engineering* **2018**, *4* (6), 831−847.

(8) Huston, R.; Butler, J. N. Standard potential of the lithium electrode in aqueous solutions. *J. Phys. Chem.* **1968**, *72* (12), 4263−4264.

(9) Perea, A.; Dontigny, M.; Zaghib, K. Safety of solid-state Li metal battery: Solid polymer versus liquid electrolyte. *J. Power Sources* **2017**, *359*, 182−185.

(10) Long, L.; Wang, S.; Xiao, M.; Meng, Y. Polymer electrolytes for lithium polymer batteries. *J. Mater. Chem. A* **2016**, *4* (26), 10038−10069.

(11) Quartarone, E.; Mustarelli, P. Electrolytes for solid-state lithium rechargeable batteries: recent advances and perspectives. *Chem. Soc. Rev.* **2011**, *40* (5), 2525−40.

(12) Yue, L.; Ma, J.; Zhang, J.; Zhao, J.; Dong, S.; Liu, Z.; Cui, G.; Chen, L. All solid-state polymer electrolytes for high-performance lithium ion batteries. *Energy Storage Materials* **2016**, *5*, 139−164.

(13) Brandell, D.; Mindemark, J.; Hernández, G. *Polymer-based Solid State Batteries*; Walter de Gruyter GmbH Location: Berlin/Boston, 2021.

(14) Mauger, A.; Julien, C. M.; Paolella, A.; Armand, M.; Zaghib, K. Building Better Batteries in the Solid State: A Review. *Materials* **2019**, *12* (23), 3892.

(15) Peters, F.; Langer, F.; Hillen, N.; Koschek, K.; Bardenhagen, I.; Schwenzel, J.; Busse, M. Correlation of Mechanical and Electrical Behavior of Polyethylene Oxide-Based Solid Electrolytes for All-Solid State Lithium-Ion Batteries. *Batteries* **2019**, *5* (1), 26.

(16) Tang, W.; Tang, S.; Zhang, C.; Ma, Q.; Xiang, Q.; Yang, Y.-W.; Luo, J. Simultaneously Enhancing the Thermal Stability, Mechanical

Modulus, and Electrochemical Performance of Solid Polymer Electrolytes by Incorporating 2D Sheets. *Adv. Energy Mater.* **2018**, *8* (24), 1800866.
(17) Rosenwinkel, M. P.; Andersson, R.; Mindemark, J.; Schönhoff, M. Coordination Effects in Polymer Electrolytes: Fast Li+ Transport by Weak Ion Binding. *J. Phys. Chem. C* **2020**, *124* (43), 23588−23596.
(18) Commarieu, B.; Paolella, A.; Collin-Martin, S.; Gagnon, C.; Vijh, A.; Guerfi, A.; Zaghib, K. Solid-to-liquid transition of polycarbonate solid electrolytes in Li-metal batteries. *J. Power Sources* **2019**, *436*, 226852.
(19) Sångeland, C.; Mogensen, R.; Brandell, D.; Mindemark, J. Stable Cycling of Sodium Metal All-Solid-State Batteries with Polycarbonate-Based Polymer Electrolytes. *ACS Appl. Polym. Mater.* **2019**, *1* (4), 825−832.
(20) Ferry, A.; Orädd, G.; Jacobsson, P. Ionic interactions and transport in a low-molecular-weight model polymer electrolyte. *J. Chem. Phys.* **1998**, *108* (17), 7426−7433.
(21) Johansson, I. L.; Brandell, D.; Mindemark, J. Mechanically Stable UV-Crosslinked Polyester-Polycarbonate Solid Polymer Electrolyte for High-Temperature Batteries. *Batteries Supercaps* **2020**, *3*, 527.
(22) Lu, Q.; He, Y. B.; Yu, Q.; Li, B.; Kaneti, Y. V.; Yao, Y.; Kang, F.; Yang, Q. H. Dendrite-Free, High-Rate, Long-Life Lithium Metal Batteries with a 3D Cross-Linked Network Polymer Electrolyte. *Adv. Mater.* **2017**, *29* (13), 1604460.
(23) Lee, T. K.; Andersson, R.; Dzulkurnain, N. A.; Hernández, G.; Mindemark, J.; Brandell, D. Polyester-ZrO2 Nanocomposite Electrolytes with High Li Transference Numbers for Ambient Temperature All-Solid-State Lithium Batteries. *Batteries Supercaps* **2021**, *4* (4), 653−662.
(24) Eriksson, T.; Mindemark, J.; Yue, M.; Brandell, D. Effects of nanoparticle addition to poly(ε-caprolactone) electrolytes: Crystallinity, conductivity and ambient temperature battery cycling. *Electrochim. Acta* **2019**, *300*, 489−496.
(25) Wang, W.; Yi, E.; Fici, A. J.; Laine, R. M.; Kieffer, J. Lithium Ion Conducting Poly(ethylene oxide)-Based Solid Electrolytes Containing Active or Passive Ceramic Nanoparticles. *J. Phys. Chem. C* **2017**, *121* (5), 2563−2573.
(26) Zhang, J.; Zhao, N.; Zhang, M.; Li, Y.; Chu, P. K.; Guo, X.; Di, Z.; Wang, X.; Li, H. Flexible and ion-conducting membrane electrolytes for solid-state lithium batteries: Dispersion of garnet nanoparticles in insulating polyethylene oxide. *Nano Energy* **2016**, *28*, 447−454.
(27) Teran, A. A.; Tang, M. H.; Mullin, S. A.; Balsara, N. P. Effect of molecular weight on conductivity of polymer electrolytes. *Solid State Ionics* **2011**, *203* (1), 18−21.
(28) Yuan, R.; Teran, A. A.; Gurevitch, I.; Mullin, S. A.; Wanakule, N. S.; Balsara, N. P. Ionic Conductivity of Low Molecular Weight Block Copolymer Electrolytes. *Macromolecules* **2013**, *46* (3), 914−921.
(29) Meabe, L.; Goujon, N.; Li, C.; Armand, M.; Forsyth, M.; Mecerreyes, D. Single-Ion Conducting Poly(Ethylene Oxide Carbonate) as Solid Polymer Electrolyte for Lithium Batteries. *Batteries Supercaps* **2020**, *3* (1), 68−75.
(30) Deng, K.; Qin, J.; Wang, S.; Ren, S.; Han, D.; Xiao, M.; Meng, Y. Effective Suppression of Lithium Dendrite Growth Using a Flexible Single-Ion Conducting Polymer Electrolyte. *Small* **2018**, *14*, 1801420.
(31) Mindemark, J.; Törmä, E.; Sun, B.; Brandell, D. Copolymers of trimethylene carbonate and ε-caprolactone as electrolytes for lithium-ion batteries. *Polymer* **2015**, *63*, 91−98.
(32) Daigle, J.-C.; Vijh, A.; Hovington, P.; Gagnon, C.; Hamel-Pâquet, J.; Verreault, S.; Turcotte, N.; Clément, D.; Guerfi, A.; Zaghib, K. Lithium battery with solid polymer electrolyte based on comb-like copolymers. *J. Power Sources* **2015**, *279*, 372−383.
(33) Nguyen, H.-D.; Kim, G.-T.; Shi, J.; Paillard, E.; Judeinstein, P.; Lyonnard, S.; Bresser, D.; Iojoiu, C. Nanostructured multi-block copolymer single-ion conductors for safer high-performance lithium batteries. *Energy Environ. Sci.* **2018**, *11* (11), 3298−3309.
(34) Hallinan, D. T.; Balsara, N. P. Polymer Electrolytes. *Annu. Rev. Mater. Res.* **2013**, *43* (1), 503−525.
(35) Ghosh, A.; Wang, C.; Kofinas, P. Block Copolymer Solid Battery Electrolyte with High Li-Ion Transference Number. *J. Electrochem. Soc.* **2010**, *157* (7), A846.
(36) Bergfelt, A.; Hernández, G.; Mogensen, R.; Lacey, M. J.; Mindemark, J.; Brandell, D.; Bowden, T. M. Mechanically Robust Yet Highly Conductive Diblock Copolymer Solid Polymer Electrolyte for Ambient Temperature Battery Applications. *ACS Appl. Polym. Mater.* **2020**, *2* (2), 939−948.
(37) Lv, Z.; Tang, Y.; Dong, S.; Zhou, Q.; Cui, G. Polyurethane-based polymer electrolytes for lithium Batteries: Advances and perspectives. *Chem. Eng. J.* **2022**, *430*, 132659.
(38) Asplund, B. Biodegradable Thermoplastic Elastomers. Doctoral Thesis, Uppsala University, Acta Universitatis Upsaliensis, 2007.
(39) Bao, J.; Qu, X.; Qi, G.; Huang, Q.; Wu, S.; Tao, C.; Gao, M.; Chen, C. Solid electrolyte based on waterborne polyurethane and poly(ethylene oxide) blend polymer for all-solid-state lithium ion batteries. *Solid State Ionics* **2018**, *320*, 55−63.
(40) Tao, C.; Gao, M.-H.; Yin, B.-H.; Li, B.; Huang, Y.-P.; Xu, G.; Bao, J.-J. A promising TPU/PEO blend polymer electrolyte for all-solid-state lithium ion batteries. *Electrochim. Acta* **2017**, *257*, 31−39.
(41) Bao, J.; Shi, G.; Tao, C.; Wang, C.; Zhu, C.; Cheng, L.; Qian, G.; Chen, C. Polycarbonate-based polyurethane as a polymer electrolyte matrix for all-solid-state lithium batteries. *J. Power Sources* **2018**, *389*, 84−92.
(42) Porcarelli, L.; Manojkumar, K.; Sardon, H.; Llorente, O.; Shaplov, A. S.; Vijayakrishna, K.; Gerbaldi, C.; Mecerreyes, D. Single Ion Conducting Polymer Electrolytes Based On Versatile Polyurethanes. *Electrochim. Acta* **2017**, *241*, 526−534.
(43) Wu, N.; Shi, Y. R.; Lang, S. Y.; Zhou, J. M.; Liang, J. Y.; Wang, W.; Tan, S. J.; Yin, Y. X.; Wen, R.; Guo, Y. G. Self-Healable Solid Polymeric Electrolytes for Stable and Flexible Lithium Metal Batteries. *Angew. Chem., Int. Ed. Engl.* **2019**, *58* (50), 18146−18149.
(44) Sun, B.; Mindemark, J.; Edström, K.; Brandell, D. Polycarbonate-based solid polymer electrolytes for Li-ion batteries. *Solid State Ionics* **2014**, *262*, 738−742.
(45) Evans, J.; Vincent, C. A.; Bruce, P. G. Electrochemical measurement of transference numbers in polymer electrolytes. *Polymer* **1987**, *28* (13), 2324−2328.
(46) Hiller, M. M.; Joost, M.; Gores, H. J.; Passerini, S.; Wiemhöfer, H. D. The influence of interface polarization on the determination of lithium transference numbers of salt in polyethylene oxide electrolytes. *Electrochim. Acta* **2013**, *114*, 21−29.
(47) Devaux, D.; Bouchet, R.; Glé, D.; Denoyel, R. Mechanism of ion transport in PEO/LiTFSI complexes: Effect of temperature, molecular weight and end groups. *Solid State Ionics* **2012**, *227*, 119−127.
(48) Timachova, K.; Watanabe, H.; Balsara, N. P. Effect of Molecular Weight and Salt Concentration on Ion Transport and the Transference Number in Polymer Electrolytes. *Macromolecules* **2015**, *48* (21), 7882−7888.
(49) Mindemark, J.; Sun, B.; Törmä, E.; Brandell, D. High-performance solid polymer electrolytes for lithium batteries operational at ambient temperature. *J. Power Sources* **2015**, *298*, 166−170.
(50) Kimura, K.; Yajima, M.; Tominaga, Y. A highly-concentrated poly(ethylene carbonate)-based electrolyte for all-solid-state Li battery working at room temperature. *Electrochem. Commun.* **2016**, *66*, 46−48.
(51) Mezger, T. G. *The Rheology Handbook: For users of rotational and oscillatory rheometers*, 4th ed.; Vincentz Network GmbH & Co. KG: Hanover, 2014.
(52) Mindemark, J.; Sobkowiak, A.; Oltean, G.; Brandell, D.; Gustafsson, T. Mechanical Stabilization of Solid Polymer Electrolytes through Gamma Irradiation. *Electrochim. Acta* **2017**, *230*, 189−195.
(53) Kim, J. Y.; Hong, S. U.; Won, J.; Kang, Y. S. Molecular Model and Analysis of Glass Transition Temperatures for Polymer−Diluent−Salt Systems. *Macromolecules* **2000**, *33* (8), 3161−3165.

https://doi.org/10.1021/acsaem.1c02942
ACS Appl. Energy Mater. 2022, 5, 407−418

(54) Pizzi, A.; Mittal, K. L. Principles of Polymer Networking and Gel Theory in Thermosetting Adhesive Formulations. In *Handbook of Adhesive Technology, Revised and Expanded*; Marcel Dekker: New York, 2003.
(55) Wang, T.-L.; Hsieh, T.-H. Effect of polyol structure and molecular weight on the thermal stability of segmented poly-(urethaneureas). *Polym. Degrad. Stab.* **1997**, *55* (1), 95−102.
(56) Thring, R. W.; Ni, P.; Aharoni, S. M. Molecular Weight Effects of the Soft Segment on the Ultimate Properties of Lignin-Derived Polyurethanes. *Int. J. Polym. Mater.* **2004**, *53* (6), 507−524.
(57) Stolwijk, N. A.; Heddier, C.; Reschke, M.; Wiencierz, M.; Bokeloh, J.; Wilde, G. Salt-Concentration Dependence of the Glass Transition Temperature in PEO−NaI and PEO−LiTFSI Polymer Electrolytes. *Macromolecules* **2013**, *46* (21), 8580−8588.
(58) Vogel, H. Das Temperaturabhaengigkeitsgesetz der Viskositaet von Fluessigkeiten. *Phys. Z.* **1921**, *22*, 646−646.
(59) Fulcher, G. S. Analysis of Recent Measurements of the Viscosity of Glasses. *J. Am. Ceram. Soc.* **1925**, *8* (6), 339−355.
(60) Tammann, G.; Hesse, W. Die Abhängigkeit der Viscosität von der Temperatur bie unterkühlten Flüssigkeiten. *J. Inorg. Gen. Chem.* **1926**, *156* (1), 245−257.
(61) Sun, B.; Mindemark, J.; Morozov, E. V.; Costa, L. T.; Bergman, M.; Johansson, P.; Fang, Y.; Furo, I.; Brandell, D. Ion transport in polycarbonate based solid polymer electrolytes: experimental and computational investigations. *Phys. Chem. Chem. Phys.* **2016**, *18* (14), 9504−9513.
(62) Sångeland, C.; Sun, B.; Brandell, D.; Berg, E. J.; Mindemark, J. Decomposition of Carbonate-Based Electrolytes: Differences and Peculiarities for Liquids vs. Polymers Observed Using Operando Gas Analysis. *Batteries Supercaps* **2021**, *4* (5), 785−790.
(63) Zhang, Z.; Yang, J.; Huang, W.; Wang, H.; Zhou, W.; Li, Y.; Li, Y.; Xu, J.; Huang, W.; Chiu, W.; Cui, Y. Cathode-Electrolyte Interphase in Lithium Batteries Revealed by Cryogenic Electron Microscopy. *Matter* **2021**, *4* (1), 302−312.
(64) Choudhury, S.; Tu, Z.; Nijamudheen, A.; Zachman, M. J.; Stalin, S.; Deng, Y.; Zhao, Q.; Vu, D.; Kourkoutis, L. F.; Mendoza-Cortes, J. L.; Archer, L. A. Stabilizing polymer electrolytes in high-voltage lithium batteries. *Nat. Commun.* **2019**, *10* (1), 3091.

https://doi.org/10.1021/acsaem.1c02942
ACS Appl. Energy Mater. 2022, 5, 407−418